Mean-field approach to magnetic ordering in highly frustrated pyrochlores

J. N. Reimers, A. J. Berlinsky, and A.-C. Shi
Institute for Materials Research, McMaster University, Hamilton, Ontario, Canada L8S 4M1
(Received 27 June 1990; revised manuscript received 17 September 1990)

The metal atoms in the pyrochlore system of compounds ($A_2B_2O_7$, where A and B are metals) form an infinite three-dimensional network of corner-sharing tetrahedra with cubic symmetry. For antiferromagnetic nearest-neighbor interactions and only B atoms magnetic, there is a very high degree of frustration, and no long-range order is predicted in the absence of further neighbor interactions. A general form of the mean-field theory is developed for dealing with n-component classical vector spins on any lattice. Calculations for the pyrochlore problem show that the Fourier modes of the system are completely degenerate for all wave vectors in the first Brillouin zone. In some cases further neighbor interactions will select the $\mathbf{q}=\mathbf{0}$ or incommensurate modes. A comparison is made with long-range order known to exist in the pyrochlore form of FeF_3. The highly degenerate ordered phases of more complicated systems, where both A and B atoms are magnetic, will also be discussed. A comparison is made of the corner-sharing tetrahedral lattice and the more familiar stacked triangular antiferromagnets, with regard to the degree of frustration in both systems. Results for the Kagomé lattice and the square lattice with crossings, which are the two-dimensional analogs of the corner-sharing tetrahedral lattice, are also briefly discussed.

INTRODUCTION

Pyrochlores have the chemical composition $A_2B_2O_7$ and crystallize in the cubic, face-centered space group $Fd\bar{3}m$, where the A and B atoms are metals located on the sites 16c and 16d of the space group. Each of the metal atoms in this system forms an infinite three-dimensional lattice of corner-sharing tetrahedra. If either of the A or B atoms is magnetic then there is a very high degree of frustration when the nearest-neighbor interactions are antiferromagnetic. A schematic diagram of the tetrahedra formed by the 16c lattice within a unit cell is shown in Fig. 1; the 16d sublattice is identical except for a spatial displacement of $(\frac{1}{2},\frac{1}{2},\frac{1}{2})$. The problem of antiferromagnetic ordering on this lattice was first considered by Anderson,[1] who predicted on qualitative grounds a very high ground-state degeneracy and that no long-range order would exist at any temperature for Ising spins. Villain reached basically the same conclusion for Heisenberg spins,[2] calling the system a "cooperative paramagnet."

This interesting lattice is also realized in spinel compounds, AB_2O_4 at the B site, and in the cubic Laves phase RMn_2 where the Mn atoms lie on the 16d site. Many of these systems undergo lattice distortions at the magnetic phase transition which will lift the degeneracy of the magnetic ground state. Neutron-diffraction experiments on a large number of the spinel compounds[3] and YMn_2 (Ref. 4) have shown significant diffuse scattering over a wide temperature range above T_c and complex magnetic order below T_c, which are both indications of magnetic frustration.

Very little is known about magnetic ordering in pyrochlore antiferromagnets, in fact, FeF_3 is the only such compound for which a low-temperature magnetic structure has been observed.[5] Here the low-temperature phase consists of four sublattices oriented along the four [111] directions. Thus any two sublattices are oriented at 109° from each other. Signs of frustration are evident at temperatures on the order of $10T_c$ where the susceptibility shows strong deviations from Curie-Weiss behavior.

Heat-capacity measurements[6] for the series of compounds $R_2M_2O_7$ (R = rare earth, $M=\mathrm{Ti,Sn,Zr,}\frac{1}{2}\{Ga^{3+}Sb^{5+}\}$) show transitions to long-range order in only a few cases, and then only at temperatures below 2 K. The remaining systems show broad features in the heat capacity which may be due to the onset of short-range order over a wide temperature range. It is reasonable to suspect that antiferromagnetic coupling between the rare-earth atoms, and therefore frustration, are in some part responsible for the observed effects.

A large amount of work has also been done on the related series of compounds $R_2M_2O_7$ [R = rare earth, M=Mo (Ref. 7), Mn (Ref. 8)]. Magnetic measurements for the Mo series show a wide range of magnetic behavior, in particular $Nd_2Mo_2O_7$ and $Sm_2Mo_2O_7$ have complex magnetization curves with two apparent critical temperatures. For R=Tb, Dy, Ho, Er, Tm, Yb, and Y, the susceptibility data indicate strong deviations from Curie-Weiss behavior and no evidence for long-range order down to 4 K. In fact $Y_2Mo_2O_7$ seems to exhibit spin-glass-like behavior[9] even though there is no evidence for structural disorder.[10] Recent susceptibility and neutron-diffraction data for $Tb_2Mo_2O_7$ (Ref. 11) are also reminiscent of spin glasses.

All of the $R_2Mn_2O_7$ compounds appear to be ferromagnetic from high-field susceptibility data;[8] however, it is still of interest to discuss the possibility of antiferromagnetic nearest-neighbor interactions for the Mn sublattice. In fact low-field susceptibility data for $Y_2Mn_2O_7$

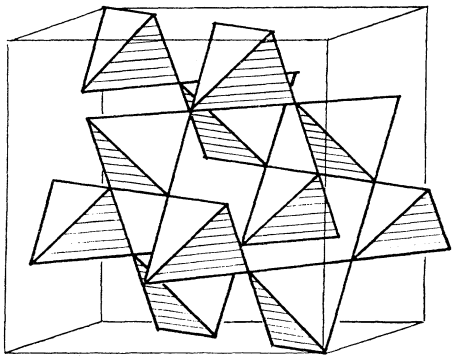

FIG. 1. The three-dimensional network of corner-sharing tetrahedra formed by one of the metal sublattices in pyrochlores. An outline of the cubic unit cell is also shown.

indicate the onset of antiferromagnetic correlations at 7 K.[12] A more complete review of the magnetic properties of oxide pyrochlores will be found in Ref. 13.

The aim of this paper is to investigate, within mean-field theory, the magnetic properties and ordered magnetic phases of $A_2B_2O_7$ systems with classical vector spins. By expressing the possible spin structures of the system in terms of Fourier components or normal modes, we will attempt to show that the frustration in these systems is characterized by the unusually large number of modes which become unstable as the temperature is lowered to T_c. These unstable modes dictate the highest-temperature ordered phase of the system.

The paper is organized as follows. In Sec. I we discuss the ground states of small clusters, their degeneracies, and their degree of frustration. The mean-field and Landau-theory formalism for n-component classical spins on general lattice systems is developed in Sec. II. In Sec. III the magnetic sublattices in pyrochlores are described in more detail and coupling matrices for a general pyrochlore system are defined. Results for models where only the B site is magnetic are presented in Sec. IV, along with a comparison of the mean-field predictions and neutron-scattering results for FeF_3 and a brief discussion of the related kagomé and square lattice with crossings. In Sec. V we discuss the ordered phases for more complicated systems where both A and B sites are magnetic.

I. SMALL CLUSTERS

A. Consideration of grounds states

It is instructive to consider small finite clusters that are frustrated, in particular, the triangle and the tetrahedron. For a cluster with $p \geq 2$ spins all interconnected with interaction $J<0$ the reduced energy per spin is

$$\begin{aligned}\frac{E}{p|J|}=e&=\frac{1}{p}\sum_{i,j=1}^{p}\mathbf{S}_i\cdot\mathbf{S}_j\\&=\frac{1}{p}\left[\sum_{i=1}^{p}\mathbf{S}_i\right]^2-\frac{1}{p}\sum_{i=1}^{p}S_i^2\\&=\frac{1}{p}\left[\sum_{i=1}^{p}\mathbf{S}_i\right]^2-1\ ,\end{aligned}\tag{1.1}$$

where the sums are unrestricted and the spins are classical n-component unit vectors. The ground state of this system has reduced energy of $e_0=-1$ and is determined by the condition

$$\sum_{i=1}^{p}\mathbf{S}_i=\mathbf{0}\ .\tag{1.2}$$

Because the spins are normalized, each spin possesses $n-1$ continuous degrees of freedom giving a total of $p(n-1)$ continuous degrees of freedom for the whole cluster. The ground-state condition (1.2) reduces the number of degrees of freedom by n, assuming the set of n conditions in (1.2) are independent, which is not always the case. A contribution of n degrees of freedom associated with the choice of a global coordinate system in spin space is also subtracted. Thus the number of internal degrees of freedom for the ground state for a cluster of p,n-component spins is

$$n_0=p(n-1)-2n\ .\tag{1.3}$$

A negative result for n_0 is merely a result of the system of equations (1.2) not being independent. It is important at this point to remember that only continuous degrees of freedom are counted and not discrete degeneracies found in all Ising systems ($n=1$) and some triangular antiferromagnets.[14] This analysis also pertains to infinite systems forming a p sublattice magnetic structure with ferromagnetic intrasublattice coupling and antiferromagnetic intersublattice coupling. Some physically realizable systems would include $p=2$ (two-sublattice antiferromagnet), 3 (triangular systems), and 4 (16c and 16d in $Fd\bar{3}m$ as well as type-I fcc antiferromagnets[15]), all having $n=1$, 2, or 3. Among these systems only the case where $p=4$ and $n=3$ has $n_0>0$. In this case there are two continuous internal degrees of freedom in the ground state which we now examine in more detail.

The general ground state for the antiferromagnetic tetrahedron (in an appropriate coordinate system) can be written as follows:

$$\begin{aligned}&\mathbf{S}_1=(0,0,1)\ ,\\&\mathbf{S}_2=(\sin\theta_2,0,\cos\theta_2)\ ,\\&\mathbf{S}_3=(\cos\phi_3\sin\theta_3,\sin\phi_3\sin\theta_3,\cos\theta_3)\ ,\\&\mathbf{S}_4=(-\sin\theta_2-\cos\phi_3\sin\theta_3,-\sin\phi_3\sin\theta_3,1-\cos\theta_2-\cos\theta_3)\ ,\end{aligned}\tag{1.4}$$

where

$$\cos\phi_3=\frac{-(\cos\theta_2-1)(\cos\theta_3-1)}{\sin\theta_2\sin\theta_3}\tag{1.5}$$

and

$$0\leq\pi-\theta_2\leq\theta_3\leq\pi\ .\tag{1.6}$$

B. Measuring frustration

Lacorre has proposed a method of gauging frustration by calculating the so-called "constraint function."[16] He defines the basis energy of the system as the sum of all pair interaction energies as if they were not frustrated,

$$E_b = \sum_{i,j=1}^{p} |J_{ij}|\,|S_i|\,|S_j| \tag{1.7}$$

$$= |J| p (p-1) , \tag{1.8}$$

thus

$$\frac{E_b}{p|J|} = e_b = p-1, \quad p \geq 2 . \tag{1.9}$$

The constraint function is now defined as the ratio of the system energy per unit cell, to its basis energy

$$F_c = \frac{E}{E_b} = \frac{e}{e_b} = \frac{-1}{p-1}, \quad p \geq 2 . \tag{1.10}$$

In general, F_c ranges from -1 (nonfrustrated) to $+1$ (fully frustrated). For the model of p antiferromagnetically coupled sublattices, the degree of frustration increases with p. According to this definition the pyrochlore system ($p=4$, $F_c=-\frac{1}{3}$) is more frustrated than the triangular lattice systems ($p=3$, $F_c=-\frac{1}{2}$). The constraint function has been discussed in more general terms by Lacorre;[16] however, this measure of frustration is only relevant to the $q=0$ mode of the system. To analyze more complicated structures it is necessary to perform a more elaborate calculation which considers all possible modes of the system in a systematic manner. The appropriate formalism for such a calculation is the Landau expansion.

II. MEAN-FIELD-THEORY FORMALISM

We consider a system with the Hamiltonian

$$\mathcal{H} = -\tfrac{1}{2} \sum_{i,j} J_{ij} \mathbf{S}_i \cdot \mathbf{S}_j - \mathbf{H} \cdot \sum_i \mathbf{S}_i , \tag{2.1}$$

where the J_{ij} are isotropic exchange interactions ($J>0$ corresponds to ferromagnetic coupling), $\mathbf{H}$ is a uniform external field, and $\mathbf{S}_i$ is an n component unit spin at lattice site i. The stability of the system is governed by the free energy which has the form

$$F = \mathrm{Tr}(\rho \mathcal{H}) + T\,\mathrm{Tr}(\rho \ln \rho) . \tag{2.2}$$

Here ρ is the full density matrix of the system which, within the mean-field approximation, is approximated by a product of single spin density matrices,

$$\rho(\{\mathbf{S}\}) = \prod_i \rho_i(\mathbf{S}_i) . \tag{2.3}$$

Following the procedure of Harris, Mouritson, and Berlinsky,[17] we substitute (2.3) into (2.2) and minimize with respect to the ρ_i, subject to the constraints (which keep the internal energy fixed)

$$\mathrm{Tr}(\rho_i) = 1 , \tag{2.4a}$$

$$\mathrm{Tr}(\rho_i \mathbf{S}_i) = \mathbf{B}_i , \tag{2.4b}$$

obtaining

$$\frac{\partial}{\partial \rho_i} \mathrm{Tr}[\rho_i \ln \rho_i - \rho_i(\lambda_i + \mathbf{A}_i \cdot \mathbf{S}_i)] = 0 \tag{2.5a}$$

or

$$\rho_i = C_i^{-1} \exp(\mathbf{A}_i \cdot \mathbf{S}_i) , \tag{2.5b}$$

where λ_i and $\mathbf{A}_i$ are Lagrange multipliers for the constraints (2.4a) and (2.4b), respectively, and C_i is determined by the normalization condition (2.4a). For n-component classical spins the trace has the form of an integral over the surface of an n-dimensional hypersphere, thus

$$C_i(A_i) = \int d\Omega \exp(\mathbf{A}_i \cdot \mathbf{S}_i) = \frac{(2\pi)^{\nu+1} I_\nu(A_i)}{A_i^\nu}, \quad \nu \geq 0 \tag{2.6}$$

where $I_\nu(A_i)$ is a modified Bessel function, $A_i = |\mathbf{A}_i|$ and $\nu = n/2 - 1$. It is also useful to obtain an expression for the order parameters $\mathbf{B}_i$

$$\mathrm{Tr}(\rho_i \mathbf{S}_i) = C_i^{-1} \int d\Omega\, \mathbf{S}_i \exp(\mathbf{A}_i \cdot \mathbf{S}_i) = \frac{\nabla_{\mathbf{A}} C_i(A_i)}{C_i(A_i)} = \hat{A}_i \frac{\dfrac{\partial C_i(A_i)}{\partial A_i}}{C_i(A_i)} ,$$

$$\mathbf{B}_i = \hat{A}_i \frac{I_{\nu+1}(A_i)}{I_\nu(A_i)} , \tag{2.7a}$$

or

$$B_i = \frac{I_{\nu+1}(A_i)}{I_\nu(A_i)} . \tag{2.7b}$$

The $\mathbf{A}_i$'s can be interpreted as local effective fields acting on the spins and are collinear with the order parameters $\mathbf{B}_i$. Substituting expressions (2.4), (2.5), and (2.7) into (2.2), one obtains an expression for the free energy of the system in terms of the order parameters $\mathbf{B}_i$,

$$F(T,\mathbf{H}) = -\tfrac{1}{2} \sum_{i,j} J_{ij} \mathbf{B}_i \cdot \mathbf{B}_j - \mathbf{H} \cdot \sum_i \mathbf{B}_i + T \sum_i (B_i \Lambda(B_i) - \ln\{C[\Lambda(B_i)]\}) , \tag{2.8}$$

$$\Lambda(B_i) = A_i . \tag{2.9}$$

The function $\Lambda(B_i)$ is the inverse of (2.7b). The stability conditions for the system can be obtained by minimizing $F(T,\mathbf{H})$ with respect to the $\mathbf{B}_i$'s or the $\mathbf{A}_i$'s. For simplicity we choose the former option, yielding the mean-field equations for this problem,

$$\nabla_{\mathbf{B}_i} F(T,\mathbf{H}) = -\mathbf{M}_i \cdot \mathbf{B}_i + T\,\mathbf{A}_i = \mathbf{0} , \tag{2.10}$$

$$\mathbf{M}_i = \sum_j J_{ij} \mathbf{B}_j + \mathbf{H} . \tag{2.11}$$

Small B_i expansions of the entropy term in (2.8) and relations (2.7) and (2.9) will be useful for a Landau expansion

$$B(A)=\frac{A}{n}-\frac{A^3}{n^2(n+2)}+2\frac{A^5}{n^3(n+2)(n+4)} -\frac{A^7(5n+12)}{n^5(n+2)^2(n+4)(n+6)}+\cdots , \tag{2.12}$$

$$A(B)=nB+\frac{n^2B^3}{n+2}+\frac{n^3(n+8)B^5}{(n+2)^2(n+4)} +\frac{n^4(n^2+14n+120)B^7}{(n+2)^3(n+4)(n+6)}+\cdots , \tag{2.13}$$

$$-S_i=\ln\left[\frac{\Gamma(n/2)}{2\sqrt{\pi^n}}\right]+\frac{nB_i^2}{2}+\frac{n^2B_i^4}{4(n+2)} +\frac{n^3(n+8)B_i^6}{6(n+2)^2(n+4)}+\cdots . \tag{2.14}$$

In order to take advantage of the translational symmetry of the lattice, we also expand the order parameters B_i in terms of Fourier components. When considering non-Bravias lattices, it is convenient to label the spins in terms of unit-cell coordinates and a sublattice index within the unit cell,

$$\mathbf{B}_i^a=\sum_{\mathbf{q}}\mathbf{B}_{\mathbf{q}}^a\exp(i\mathbf{q}\cdot\mathbf{R}_i) , \tag{2.15}$$

$$J_{R_{ij}}^{ab}=\frac{1}{N}\sum_{\mathbf{q}}J_{\mathbf{q}}^{ab}\exp(-i\mathbf{q}\cdot\mathbf{R}_{ij}) . \tag{2.16}$$

Here i and j refer to unit cells and a and b refer to sublattices. To obtain the Landau theory we substitute (2.14), (2.15), and (2.16) into (2.8). Keeping terms up to fourth order in the order parameters, the free energy *per unit cell* is

$$\begin{aligned}F(T,\mathbf{H})/N&=f(T,\mathbf{H})\\&=pT\ln\left[\frac{\Gamma(n/2)}{2\sqrt{\pi^n}}\right]-\sum_a\mathbf{H}\cdot\mathbf{B}_0^a\\&\quad+\tfrac{1}{2}\sum_{\mathbf{q}}\sum_{ab}\mathbf{B}_{\mathbf{q}}^a\cdot\mathbf{B}_{-\mathbf{q}}^b(nT\delta^{ab}-J_{\mathbf{q}}^{ab})\\&\quad+\frac{Tn^2}{4(n+2)}\sum_a\sum_{\{\mathbf{q}\}}'(\mathbf{B}_{\mathbf{q}_1}^a\cdot\mathbf{B}_{\mathbf{q}_2}^a)(\mathbf{B}_{\mathbf{q}_3}^a\cdot\mathbf{B}_{\mathbf{q}_4}^a) ,\end{aligned} \tag{2.17}$$

where

$$\sum_{\{\mathbf{q}\}}'=\sum_{\mathbf{q}_1,\mathbf{q}_2,\mathbf{q}_3,\mathbf{q}_4}\delta(\mathbf{q}_1+\mathbf{q}_2+\mathbf{q}_3+\mathbf{q}_4)$$

for a system with N unit cells and p spins per unit cell, and δ^{ab} is a Kronecker delta. Diagonalizing the second-order term requires transforming to normal modes of the system

$$\mathbf{B}_{\mathbf{q}}^a=\sum_i U_{\mathbf{q}}^{ai}\mathbf{\Phi}_{\mathbf{q}}^i , \tag{2.18}$$

where $U_{\mathbf{q}}$ is a unitary matrix that diagonalizes $J_{\mathbf{q}}$ with eigenvalues $\lambda_{\mathbf{q}}$

$$\sum_b J_{\mathbf{q}}^{ab}U_{\mathbf{q}}^{bi}=\lambda_{\mathbf{q}}^iU_{\mathbf{q}}^{ai} . \tag{2.19}$$

The convention that indices (ab) label sublattices and indices $(ijkl)$ label the normal modes will be used. Thus $U_{\mathbf{q}}^{ai}$ is the ath component of the ith eigenvector of $J_{\mathbf{q}}^{ab}$. In general, diagonalizing the second-order term has the effect of complicating the form of the fourth-order term in the expansion

$$\begin{aligned}f(T,\mathbf{H})&=pT\ln\left[\frac{\Gamma(n/2)}{2\sqrt{\pi^n}}\right]-\sum_{ai}U_0^{ai}\mathbf{H}\cdot\mathbf{\Phi}_0^i\\&\quad+\tfrac{1}{2}\sum_{\mathbf{q}}\sum_i\mathbf{\Phi}_{\mathbf{q}}^i\cdot\mathbf{\Phi}_{-\mathbf{q}}^i(nT-\lambda_{\mathbf{q}}^i)\\&\quad+\frac{Tn^2}{4(n+2)}\sum_{\{\mathbf{q}\}}'\sum_{ijkl}(\mathbf{\Phi}_{\mathbf{q}_1}^i\cdot\mathbf{\Phi}_{\mathbf{q}_2}^j)(\mathbf{\Phi}_{\mathbf{q}_3}^k\cdot\mathbf{\Phi}_{\mathbf{q}_4}^l)\\&\qquad\times\sum_a U_{\mathbf{q}_1}^{ai}U_{\mathbf{q}_2}^{aj}U_{\mathbf{q}_3}^{ak}U_{\mathbf{q}_4}^{al} .\end{aligned} \tag{2.20}$$

Obviously the characteristic physics of the system is contained in the $\lambda_{\mathbf{q}}^i$ and the $U_{\mathbf{q}}^{ai}$. The first ordered state of the system will occur at a temperature

$$T_c=\frac{1}{n}\max_{\mathbf{q},i}\{\lambda_{\mathbf{q}}^i\} , \tag{2.21}$$

where max { } indicates a global maximum for all i and $\mathbf{q}$.

III. APPLICATION TO PYROCHLORES

A. The pyrochlore lattice

In order to simplify the calculations somewhat, the system will be described in a nonstandard rhombohedral setting with a unit cell having one-quarter the volume of the cubic cell. The lattice vectors of the two systems are related by

$$\begin{bmatrix}\mathbf{a}\\\mathbf{b}\\\mathbf{c}\end{bmatrix}^{\text{rhom}}=\begin{bmatrix}0&\frac{1}{2}&\frac{1}{2}\\\frac{1}{2}&0&\frac{1}{2}\\\frac{1}{2}&\frac{1}{2}&0\end{bmatrix}\begin{bmatrix}\mathbf{a}\\\mathbf{b}\\\mathbf{c}\end{bmatrix}^{\text{cubic}} . \tag{3.1}$$

The advantage of the rhombohedral basis is that there are only eight metal atoms per unit cell (four of the type 16c and four of the type 16d), as opposed to 32 per cell in the cubic system. The corresponding space group is $R\bar{3}m$, which is a subgroup of $Fd\bar{3}m$. Thus the rhombohedral representation has the disadvantage that some of the inherent symmetry is hidden. Table I shows a list of metal positions for both systems along with their nearest neighbors (NN's) listed by atom number. The factor of 2 in front of each list of NN's indicates that there are two of each type of NN, which are related by spatial inversion.

B. The general NN coupling matrix

From the Fourier transform of (2.16) and the information in Table I, one can calculate the matrix $J_{\mathbf{q}}^{ab}$ for the general pyrochlore problem with nearest-neighbor interactions. We first define

TABLE I. Pyrochlore metal atom positions in rhombohedral and cubic basis, nearest neighbors are listed by atom number. FC stands for the face-centering operation $(0,0,0;0,\frac{1}{2},\frac{1}{2};\frac{1}{2},0,\frac{1}{2};\frac{1}{2},\frac{1}{2},0)$.

Site	Atom No.	Position Rhom	Cubic	Nearest neighbors
16c	1	(0,0,0)	(0,0,0)+FC	2×(2,3,4,6,7,8)
16c	2	$(\frac{1}{2},0,0)$	$(0,\frac{1}{4},\frac{1}{4})$+FC	2×(1,3,4,5,7,8)
16c	3	$(0,\frac{1}{2},0)$	$(\frac{1}{4},0,\frac{1}{4})$+FC	2×(1,2,4,5,6,8)
16c	4	$(0,0,\frac{1}{2})$	$(\frac{1}{4},\frac{1}{4},0)$+FC	2×(1,2,3,5,6,7)
16d	5	$(\frac{1}{2},\frac{1}{2},\frac{1}{2})$	$(\frac{1}{2},\frac{1}{2},\frac{1}{2})$+FC	2×(2,3,4,6,7,8)
16d	6	$(0,\frac{1}{2},\frac{1}{2})$	$(\frac{1}{2},\frac{1}{4},\frac{1}{4})$+FC	2×(1,3,4,5,7,8)
16d	7	$(\frac{1}{2},0,\frac{1}{2})$	$(\frac{1}{4},\frac{1}{2},\frac{1}{4})$+FC	2×(1,2,4,5,6,8)
16d	8	$(\frac{1}{2},\frac{1}{2},0)$	$(\frac{1}{4},\frac{1}{4},\frac{1}{2})$+FC	2×(1,2,3,5,6,7)

$$\mathcal{J}_{\text{intra}}=2\begin{bmatrix} 0 & \cos(q_x) & \cos(q_y) & \cos(q_z) \\ \cos(q_x) & 0 & \cos(q_x-q_y) & \cos(q_z-q_x) \\ \cos(q_y) & \cos(q_x-q_y) & 0 & \cos(q_y-q_z) \\ \cos(q_z) & \cos(q_z-q_x) & \cos(q_y-q_z) & 0 \end{bmatrix},$$

$$\mathcal{J}_{\text{inter}}=2\begin{bmatrix} 0 & \cos(q_y-q_z) & \cos(q_z-q_x) & \cos(q_x-q_y) \\ \cos(q_y-q_z) & 0 & \cos(q_z) & \cos(q_y) \\ \cos(q_z-q_x) & \cos(q_z) & 0 & \cos(q_x) \\ \cos(q_x-q_y) & \cos(q_y) & \cos(q_x) & 0 \end{bmatrix},$$

which are, respectively, the intrasublattice and the intersublattice couplings matrices for the 16c and the 16d sites. The full coupling matrix now has the form

$$J_{\mathbf{q}}^{ab}=\begin{bmatrix} J_1 & \mathcal{J}_{\text{intra}} & J_{12} & \mathcal{J}_{\text{inter}} \\ J_{12} & \mathcal{J}_{\text{inter}} & J_2 & \mathcal{J}_{\text{intra}} \end{bmatrix}, \tag{3.2}$$

where J_1 and J_2 are couplings for metal atoms within the 16c and 16d sublattices, respectively, and J_{12} is the coupling between 16c and 16d.

In the next section systems will be considered in which only one of the metal atoms is magnetic. This is applicable to materials such as FeF_3,[5] $Y_2Mo_2O_7$,[7,9] and $Y_2Mn_2O_7$,[8] where the yttrium atoms are diamagnetic.

IV. ONE MAGNETIC SUBLATTICE (ONE OF *A* OR *B* IS MAGNETIC)

A. Ordering wave vectors

For this model there are four magnetic atoms per unit cell and

$$J_{\mathbf{q}}^{ab}=J_1\mathcal{J}_{\text{intra}}\ , \tag{4.1}$$

which can be diagonalized explicitly. By defining

$$\begin{aligned} Q=\tfrac{1}{2}[&\cos(2q_x)+\cos(2q_y)+\cos(2q_z) \\ &+\cos(2q_x-2q_y)+\cos(2q_y-2q_z) \\ &+\cos(2q_z-2q_x)]\ , \end{aligned} \tag{4.2}$$

we have

$$\begin{aligned} \lambda_{\mathbf{q}}^1&=\lambda_{\mathbf{q}}^2=-2J_1\ , \\ \lambda_{\mathbf{q}}^3&=2J_1(1-\sqrt{1+Q})\ , \\ \lambda_{\mathbf{q}}^4&=2J_1(1+\sqrt{1+Q})\ . \end{aligned} \tag{4.3}$$

Note that λ^1 and λ^2 are completely independent of $\mathbf{q}$ and that these are the maximal eigenvalues for the system when $J_1<0$. Dispersion curves for the four modes are shown in Fig. 2, from which one can see that mode 3 is also degenerate with 1 and 2 at $\mathbf{q}=\mathbf{0}$. Bertaut was aware of this high degree of degeneracy but only along certain high symmetry directions in $\mathbf{q}$ space.[18] Thus mean-field theory predicts a special temperature, $T_c=\frac{2}{3}|J_1|$ below which the system preferentially samples modes 1 and 2, i.e., a phase space with half the dimensionality of the high-temperature phase space. The heat capacity for this system should show an entropy change of k ln2 over a rather broad temperature range. Whether or not this entropy change will appear in the form of a Schottky anomaly is not yet clear.

In light of this information one can see that any sort of long-range order [within the mean-field (MF) approximation] in this system can only arise from the presence of further neighbor interactions, such as second neighbor exchange, dipole forces, or perhaps an external field. It is therefore interesting to examine the effects of further

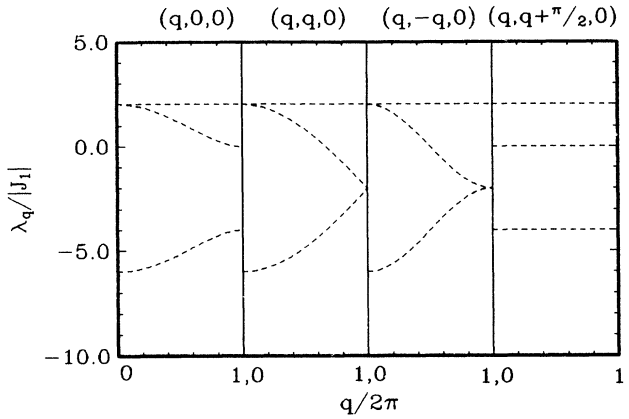

FIG. 2. Dispersion curves along certain symmetry directions, for one-sublattice pyrochlore systems with only NN exchange interactions. The unstable or critical modes will have the largest eigenvalue λ_q which is measured in units of J_1 which is the NN coupling constant.

neighbor interactions by considering the first four coordination shells. Table II shows the type of neighbors and their distances for atom 1. The neighbors for atoms 2, 3, and 4 are easily obtained by permuting atom labels. The J_q^{ab} matrix now becomes significantly more complicated and the matrix elements are written out explicitly in Appendix A. In order to get a qualitative idea of the effects of these weak further neighbor interactions, it is useful to look at how the eigenvalues for the four modes behave for the six exchange models listed in Table III. Dispersion curves for these models are shown in Figs. 3, 4, and 5. Model I_a will order in an incommensurate phase with wave vector $(q_0,-q_0,0)$ or $(q_0,q_0,2q_0)$, where q_0 is an irrational function of J_1/J_2. By permuting the indices one can see that the two points above are each sixfold degenerate, making a total of 12 independent ordering wave vectors in the first zone. Models I_b and II_a order with wave vector (0,0,0), where three out of the four modes are degenerate. This corresponds to the type of ordering observed in FeF_3, as determined by neutron diffraction, which will be discussed further in the next section. The last three models have critical modes which are dispersionless along certain symmetry directions. Thus no long-range order is expected for these models (within the MF approximation).

Figures 6(a)–6(c) show the ordering wave vectors in the

TABLE II. Neighbors for one-sublattice pyrochlores in the first four coordination shells with distances (in units of rhombohedral cell edge) and exchange constants.

Shell No.	Neighbors	Distance/a_{rhom}	Coupling constant
1	2(2,3,4)	1/2	J_1
2	4(2,3,4)	$\sqrt{3/2}$	J_2
3	12(1)	1	J_3
4	4(2,3,4)	$\sqrt{5/2}$	J_4

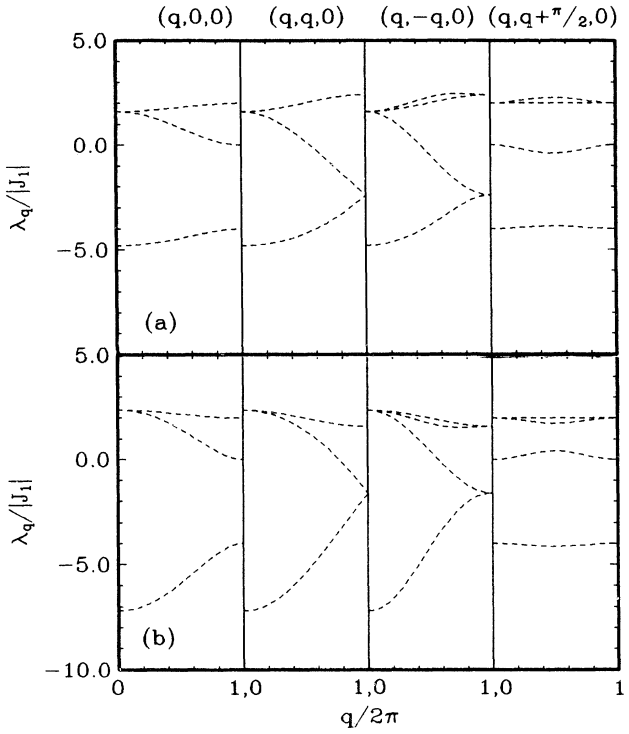

FIG. 3. As in Fig. 2 with the addition of a small second-neighbor interaction. $J_2>0$ in a and $J_2<0$ in b.

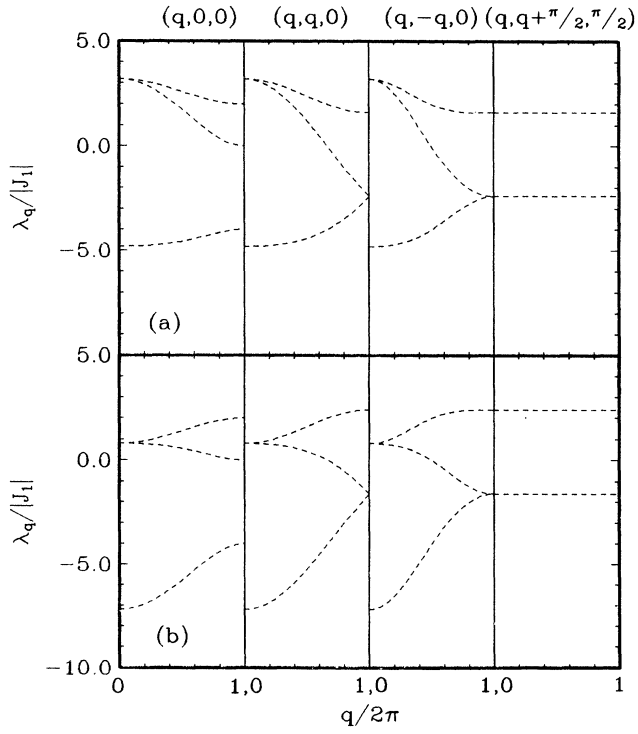

FIG. 4. As in Fig. 2 with the addition of a small third-neighbor interaction. $J_3>0$ in a and $J_3<0$ in b.

TABLE III. Six different exchange models for which dispersion curves are shown in Figs. 3, 4, and 5.

Model	J_1	J_2	J_3	J_4	Fig.
I_a	-1	>0	0	0	3(a)
I_b	-1	<0	0	0	3(b)
II_a	-1	0	>0	0	4(a)
II_b	-1	0	<0	0	4(b)
III_a	-1	0	0	>0	5(a)
III_b	-1	0	0	<0	5(b)

coupling constant space J_2 and J_3 for $J_1=-1$ and three different choices of J_4. In the $(2q,q,q)$ and $(0,q,q)$ regions the critical modes are, in general, incommensurate with finite degeneracy. Dotted lines indicate regions where the system is continuously unstable along certain directions in $\mathbf{q}$ space with infinite degeneracy and therefore no long-range order. Note that for consistency all $\mathbf{q}$ vectors discussed in this work are in the rhombohedral basis. Table IV lists all ordering wave vectors in both systems, as well as the associated multiplicities required by cubic symmetry. Unstable modes characterized by $\mathbf{q}=(2q,q,q)$ are actually 12-fold degenerate, corresponding to the star of $(q,q,0)$ directions in the cubic basis, i.e., directions $(2q,q,q)$ and $(0,q,-q)$ in the rhombohedral basis are equivalent by symmetry.

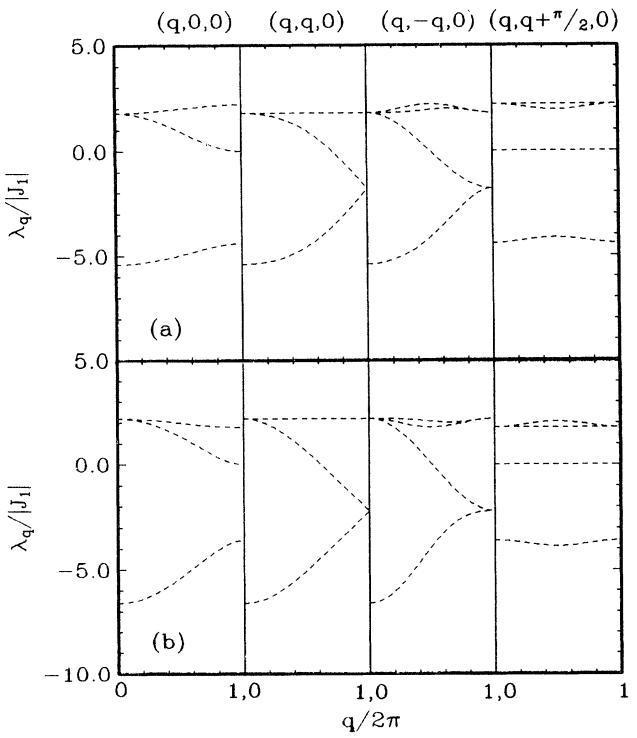

FIG. 5. As in Fig. 2 with the addition of a small fourth-neighbor interaction. $J_4>0$ in a and $J_4<0$ in b.

B. Landau theory for $\mathbf{q}=0$ (one magnetic sublattice)

The normal modes of J_0^{ab} are listed in Table V and the critical temperature at $\mathbf{H}=\mathbf{0}$ is

$$T_c=-\frac{1}{n}2(J_1+2J_2-6J_3+2J_4)\ . \tag{4.4}$$

It is important to remember that $J_1<0$, and one expects that $|J_1|\gg|J_2|$ and $|J_1|\gg|J_3|$. Substituting the information in Table V into expression (2.20) and considering only the $\mathbf{q}=0$ terms in the summations, we obtain the Landau free energy for this model

$$\begin{aligned} f=&\mu_0-2\mathbf{H}\cdot\mathbf{\Phi}_4+\tfrac{1}{2}r_0m^2+\tfrac{1}{2}r_1\Phi_4^2 \\ &+\tfrac{1}{4}u[(m^2+\Phi_4^2)^2+4(a^2+b^2+c^2)] \\ &+\tfrac{1}{6}v[(m^2+\Phi_4^2)^3+12(m^2+\Phi_4^2)(a^2+b^2+c^2) \\ &+48abc]+\cdots\ , \end{aligned} \tag{4.5}$$

where

$$\mu_0=4T\ln\left[\frac{\Gamma(n/2)}{2\sqrt{\pi}^n}\right]\ , \tag{4.6}$$

$$r_0=n(T-T_c)\ , \tag{4.7a}$$

$$r_1=n(T+3T_c)-48J_3\ , \tag{4.7b}$$

$$u=\frac{Tn^2}{4(n+2)}\ , \tag{4.8a}$$

$$v=\frac{Tn^3(n+8)}{16n(n+2)^2(n+4)}\ , \tag{4.8b}$$

$$m^2=\Phi_1^2+\Phi_2^2+\Phi_3^2\ , \tag{4.9}$$

$$a=\mathbf{\Phi}_1\cdot\mathbf{\Phi}_2+\mathbf{\Phi}_3\cdot\mathbf{\Phi}_4\ , \tag{4.10a}$$

$$b=\mathbf{\Phi}_1\cdot\mathbf{\Phi}_3+\mathbf{\Phi}_2\cdot\mathbf{\Phi}_4\ , \tag{4.10b}$$

$$c=\mathbf{\Phi}_1\cdot\mathbf{\Phi}_4+\mathbf{\Phi}_2\cdot\mathbf{\Phi}_3\ . \tag{4.10c}$$

TABLE IV. Relevant $\mathbf{q}$ vectors in rhombohedral and cubic basis and their multiplicities.

Rhombohedral	Cubic	Multiplicity
(0,0,0)	(0,0,0)	1
$(0,q,q)$	$(2q,0,0)$	6
$(2q,q,q)$	$(0,2q,2q)$	6
$(0,q,-q)$	$(0,-2q,2q)$	6
(0,1/2,1/2)	(1,0,0)	6

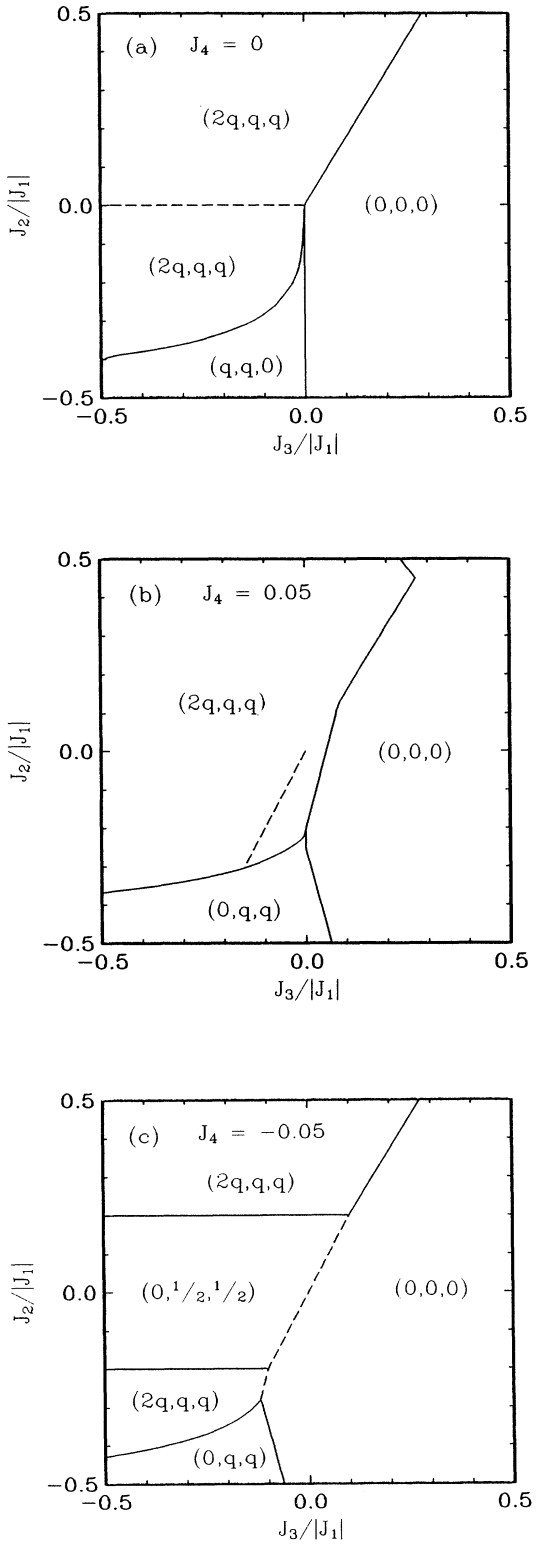

FIG. 6. Ordering wave vectors in the coupling parameter space J_3 and J_2 with $J_1=-1$ and $J_4=0$ in a, $J_4=0.05$ in b, and $J_4=-0.05$ in c. Along the dashed line the system is continuously degenerate and critical along the $(q,q+\pi/2,\pi/2)$ direction.

TABLE V. Eigenvectors and eigenvalues of the coupling matrix J_0^{ab} for one-sublattice pyrochlores.

Eigenvectors	Eigenvalues
$\Psi_1=\frac{1}{2}(1,1,-1,-1)$	$-2(J_1+2J_2-6J_3+2J_4)$
$\Psi_2=\frac{1}{2}(1,-1,1,-1)$	$-2(J_1+2J_2-6J_3+2J_4)$
$\Psi_3=\frac{1}{2}(1,-1,-1,1)$	$-2(J_1+2J_2-6J_3+2J_4)$
$\Psi_4=\frac{1}{2}(1,1,1,1)$	$6(J_1+2J_2+2J_3+2J_4)$

One can see right away that the direction of Φ_4 is determined by the external field and minimizing with respect to a, b, and c gives the conditions

$$a=b=c=0 . \tag{4.11}$$

Equations (4.11) and (4.9) impose four constraints on Φ_1, Φ_2, and Φ_3 leaving $3n-4$ degrees of freedom. Thus there is no restriction on the relative magnitudes of Φ_1, Φ_2, and Φ_3 (which for $n=3$ corresponds to the internal two-dimensional degeneracy mentioned in Sec. I) and also no restriction that one of the modes must be parallel to Φ_4 for $n\geq 3$. Also note that only r_0 is critical and not r_1. The sixth-order term has been included in order to check for tricritical behavior. Setting Φ_4 parallel to $\mathbf{H}$ and imposing condition (4.11), the Landau free energy is expressed in terms of the two variables m and Φ_4, where m should be interpreted as the order parameter for the antiferromagnetism and Φ_4 the higher energy noncritical ferromagnetic mode that couples to the external field

$$f=\mu_0-2H\Phi_4+\tfrac{1}{2}(r_0m^2+r_1\Phi_4^2)+\tfrac{1}{4}u(m^2+\Phi_4^2)^2 +\tfrac{1}{6}v(m^2+\Phi_4^2)^3+\cdots \tag{4.12}$$

with equilibrium conditions

$$[r_0+u(m^2+\Phi_4^2)+v(m^2+\Phi_4^2)^2]m=0 , \tag{4.13}$$

$$[r_1+u(m^2+\Phi_4^2)+v(m^2+\Phi_4^2)^2]\Phi_4=2H . \tag{4.14}$$

In the paramagnetic region where $m=0$ we have

$$\Phi_4=2\frac{H}{r_1}\left[1-\frac{u}{r_1}\left[\frac{2H}{r_1}\right]^2-\frac{v}{r_1}\left[\frac{2H}{r_1}\right]^4+\cdots\right] , \tag{4.15}$$

and from (4.13) and (4.14) in the ordered regime

$$\Phi_4=\frac{2H}{(r_1-r_0)}=\frac{H}{2(nT_c-12J_3)}=h , \tag{4.16}$$

which is independent of temperature and exact to all orders in $(m^2+\Phi_4^2)$ within the mean-field approximation as explained in more detail in Appendix B. We have also defined h which is the reduced field for the system. When (4.16) is substituted into (4.12) the second-and fourth-order coefficients in m are, respectively,

$$\tfrac{1}{2}(r_0+uh^2+vh^4) , \tag{4.17}$$

$$\tfrac{1}{4}(u+2vh^2) . \tag{4.18}$$

The fourth-order coefficient is positive definite and there-

fore no tricritical point exists within the mean-field approximation. Setting (4.17) equal to zero determines a line of second-order phase transitions in the (H,T) plane. Neglecting the v term we have

$$h=2\left[\frac{T_c-T}{T}\frac{n+2}{n}\right]^{1/2}, \tag{4.19}$$

which presumably saturates at low temperature due to the higher-order terms in the Landau expansion. At zero temperature

$$\sum_i B_i^2=\sum_i \Phi_i^2=m^2+\Phi_4^2=4 . \tag{4.20}$$

Substituting (4.16) into (4.20) and setting $m=0$ defines the critical field at zero temperature

$$h_c=2 , \tag{4.21a}$$

or

$$H_c=4(nT_c-12J_3) . \tag{4.21b}$$

Figure 7 shows the mean-field phase diagram for $\mathbf{q}=0$ systems.

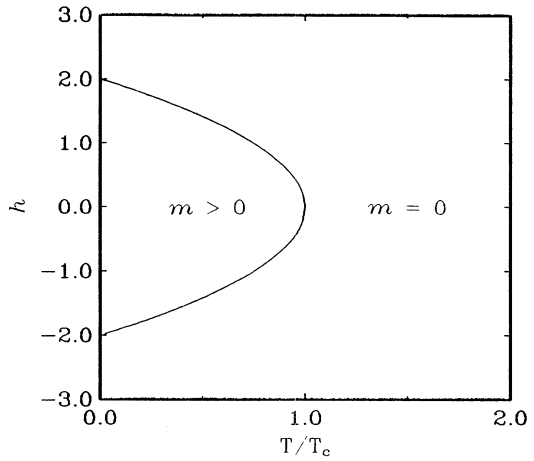

FIG. 7. (H,T) phase diagram for the $\mathbf{q}=\mathbf{0}$ systems with $J_1<0$. h is defined in (4.16), T_c in (4.4), and m is the order parameter for modes 1, 2, and 3. The solid line indicates a line of second-order phase transitions.

C. Neutron scattering for q=0 systems

The general structure factor for magnetic neutron scattering at reciprocal-lattice point (h,k,l) is

$$\mathbf{F}_{hkl}=\sum_a \mathbf{S}_{a\perp}\exp[2\pi i(hx+ky+lz)] , \tag{4.22}$$

where $\mathbf{S}_{a\perp}=\mathbf{S}_a-\hat{e}(\hat{\mathbf{e}}\cdot\mathbf{S})$ is the component of the spin, at (x,y,z), perpendicular to the scattering vector (h,k,l), and $\hat{\mathbf{e}}$ is the unit scattering vector. Working with the cubic unit cell, the structure factor for one sublattice pyrochlores with a $\mathbf{q}=0$ magnetic structure is

$$\mathbf{F}_{hkl}=\left[\mathbf{S}_{1\perp}+\mathbf{S}_{2\perp}\exp\left[i\frac{\pi}{2}(k+1)\right]+\mathbf{S}_{3\perp}\exp\left[i\frac{\pi}{2}(l+h)\right]+\mathbf{S}_{4\perp}\exp\left[i\frac{\pi}{2}(h+k)\right]\right]$$
$$\times(1+\exp[i\pi(k+l)]+\exp[i\pi(l+h)]+\exp[i\pi(h+k)]) . \tag{4.23}$$

The second factor is a result of face centering and imposes the usual constraints on h, k, and l. Ferry *et al.*[5] have proposed the following spin structure for FeF_3 based on powder diffraction:

$$\begin{aligned}&\mathbf{S}_1 \text{ along } (1,1,1) ,\\ &\mathbf{S}_2 \text{ along } (-1,1,1) ,\\ &\mathbf{S}_3 \text{ along } (1,-1,1) ,\\ &\mathbf{S}_4 \text{ along } (1,1,-1) .\end{aligned} \tag{4.24}$$

The magnetic (1,1,1) reflection in FeF_3 was absent which means for a powder that $\mathbf{F}_{1,1,1}=\mathbf{F}_{-1,1,1}=\mathbf{F}_{1,-1,1}=\mathbf{F}_{1,1,-1}=\mathbf{0}$. One can solve this system of equations explicitly and show that indeed (4.24) is the only possible spin structure. In terms of the normal modes we have

$$\begin{aligned}\mathbf{\Phi}_1&=\frac{1}{\sqrt{3}}(m,0,0) ,\\ \mathbf{\Phi}_2&=\frac{1}{\sqrt{3}}(0,m,0) ,\\ \mathbf{\Phi}_3&=\frac{1}{\sqrt{3}}(0,0,m) ,\end{aligned} \tag{4.25}$$

which is consistent with but much more restrictive than (4.9), (4.10), and (4.11). There must therefore be some anisotropy in FeF_3 that breaks the five-dimensional degeneracy of the ordered state predicted by mean-field theory. This uniaxial anisotropy is consistent with local site symmetry of the Fe^{3+} ions, as dictated by the space-group symmetry. In principle, one should be able to determine from powder neutron diffraction the magnitudes and directions of $\mathbf{\Phi}_1$, $\mathbf{\Phi}_2$, and $\mathbf{\Phi}_3$ for any $\mathbf{q}=0$ system.

D. Kagomé lattice and square lattice with crossings (Ref. 19)

By removing the third axis in the rhombohedral description of the corner-sharing tetrahedral lattice, one obtains the corresponding two-dimensional analog with basis vectors oriented at 60° and atoms at (0,0), $(\frac{1}{2},0)$, and $(0,\frac{1}{2})$ which is the Kagomé lattice. The corner-sharing tetrahedral lattice can be generated by stacking kagomé lattices along a (111) direction. The coupling matrix is a 3×3 version of $\mathcal{J}_{\text{intra}}$ with eigenvalues

$$\lambda_{\mathbf{q}}^1 = -2J_1 ,$$
$$\lambda_{\mathbf{q}}^2 = J_1(1-\sqrt{3+Q'}) , \tag{4.26}$$
$$\lambda_{\mathbf{q}}^3 = J_1(1+\sqrt{3+Q'}) ,$$
$$Q' = [\cos(2q_x)+\cos(2q_y)+\cos(2q_x-2q_y)] . \tag{4.27}$$

This is virtually the same as the three-dimensional (3D) case except that the **q**-independent mode is now nondegenerate.

If one looks at the corner-sharing tetrahedral lattice along one of cubic (100) directions, the square lattice with crossings appears. This is now a two sublattice system with the following coupling matrix and eigenvalues:

$$J_{\mathbf{q}}^{ab} = 2J \begin{bmatrix} \cos(2q_x) & 2\cos(q_x)\cos(q_y) \\ 2\cos(q_x)\cos(q_y) & \cos(2q_y) \end{bmatrix} , \tag{4.28}$$

$$\lambda_{\mathbf{q}}^1 = -2J ,$$
$$\lambda_{\mathbf{q}}^2 = 2J[1+\cos(2q_x)+\cos(2q_y)] , \tag{4.29}$$

yet again we have a completly dispersionless mode.

Thus no long-range order is predicted on either lattice within mean-field theory. These results are not surprising as the Kagomé lattice can be thought of as a corner-sharing triangular lattice, which is a natural two-dimensional (2D) extension of the 3D corner-sharing tetrahedral lattice. Similarly the square lattice with crossings can be thought of as a 2D sheet of corner-sharing tetrahedra, and is therefore just as frustrated as the 3D analog. It seems that antiferromagnets, formed by triangles or tetrahedra that only shape corners, are so sparsely connected that magnetic correlations can only communicate over short distances. Edge-sharing analogs would be the regular triangular lattice (edge-sharing triangles) and the face-centered-cubic lattice (edge-sharing tetrahedra), which both exhibit long-range order for NN antiferromagnetic interactions. This is understandable since edge sharing allows a higher degree of connectivity. Liebmann has discussed both of these 2D lattices in more detail in his book.[19] He finds very high ground-state degeneracies and no long-range order for antiferromagnetic Ising models on both lattices.

V. TWO MAGNETIC SUBLATTICES (BOTH *A* AND *B* ARE MAGNETIC)

A. Ordering wave vectors

For this problem we are dealing with an 8×8 coupling matrix as defined in (3.2) and a three-dimensional coupling parameter space spanned by J_1, J_2, and J_{12}. The effects of further neighbor interactions will not be considered here. In general the magnetic species on the two sublattices will have different moments which can be absorbed into the J's in such a way that all spins are still unit vectors. Figures 8(a) and 8(b) show maps in parameter space of J_2 and J_{12} for $J_1=0$ and $J_1=-1$, respectively, which covers all cases of interest. The phase diagram is seen to be invariant under changes in the sign of J_{12}. As before there are large regions where the $\mathbf{q}=0$ mode becomes ordered below T_c, and also regions of $(2q,q,q)$ incommensurate phases. The dotted lines along $J_{12}=0$ in both diagrams indicate regions where the whole zone is degenerate. This stems from the fact that the two sublattices are decoupled and thus have the **q**-independent eigenvalues shown in (4.3). Of particular interest is the large region in Fig. 8(b) where the system is degenerate along the $(0,q,q)$ direction. Again one expects no long-range order for such model systems.

B. Landau theory for $\mathbf{q}=0$ (two magnetic sublattices)

Again we list the eigenvalues and eigenvectors of J_0^{ab} in Table VI where

$$\alpha = \frac{J_1+J_2}{2} , \tag{5.1}$$
$$\beta = \frac{J_{12}}{|J_{12}|}\left[\left[\frac{J_1-J_2}{2}\right]^2+J_{12}^2\right]^{1/2} , \tag{5.2}$$

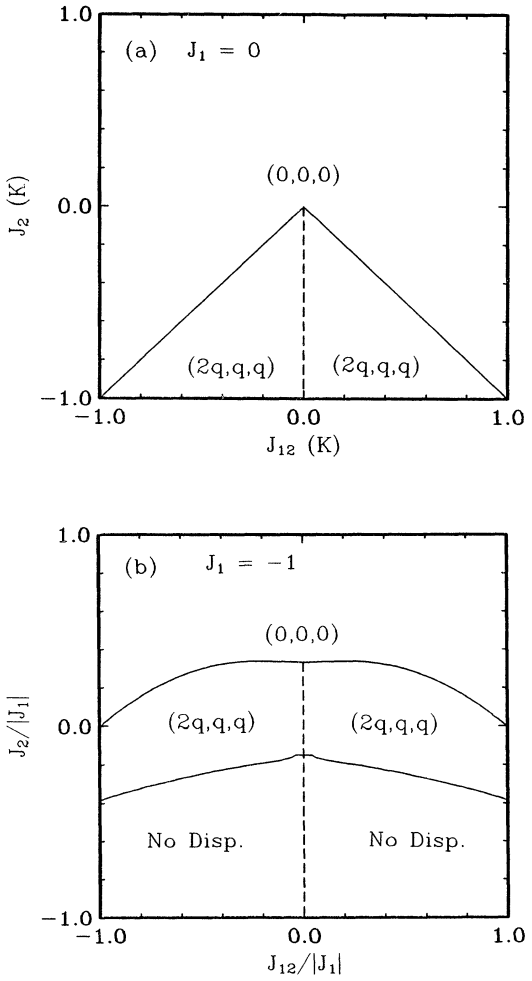

FIG. 8. Ordering wave vectors in the coupling parameter space J_2 and J_{12} with $J_1=0$ in *a* and $J_1=-1$ in *b* for two-sublattice pyrochlores with NN interactions. Along the dashed line the system is continuously degenerate and critical throughout the whole zone. "No Disp." indicates that the system is continuously degenerate along the $(0,q,q)$ directions.

TABLE VI. Eigenvectors and eigenvalues of the coupling matrix J_0^{ab} for two-sublattice pyrochlores. α, β, and ε are defined in the text.

Eigenvectors	Eigenvalues
$\Psi_1=\left[\varepsilon,\varepsilon,\varepsilon,\varepsilon,\frac{1}{\varepsilon},\frac{1}{\varepsilon},\frac{1}{\varepsilon},\frac{1}{\varepsilon}\right]$	$3(\alpha+\beta)$
$\Psi_2=\left[\frac{1}{\varepsilon},\frac{1}{\varepsilon},\frac{1}{\varepsilon},\frac{1}{\varepsilon},-\varepsilon,-\varepsilon,-\varepsilon,-\varepsilon\right]$	$3(\alpha-\beta)$
$\Psi_3=\left[\varepsilon,\varepsilon,-\varepsilon,-\varepsilon,\frac{1}{\varepsilon},\frac{1}{\varepsilon},-\frac{1}{\varepsilon},-\frac{1}{\varepsilon}\right]$	$-(\alpha+\beta)$
$\Psi_4=\left[\varepsilon,-\varepsilon,\varepsilon,-\varepsilon,\frac{1}{\varepsilon},-\frac{1}{\varepsilon},\frac{1}{\varepsilon},-\frac{1}{\varepsilon}\right]$	$-(\alpha+\beta)$
$\Psi_5=\left[\varepsilon,-\varepsilon,-\varepsilon,\varepsilon,\frac{1}{\varepsilon},-\frac{1}{\varepsilon},-\frac{1}{\varepsilon},\frac{1}{\varepsilon}\right]$	$-(\alpha+\beta)$
$\Psi_6=\left[\frac{1}{\varepsilon},\frac{1}{\varepsilon},-\frac{1}{\varepsilon},-\frac{1}{\varepsilon},-\varepsilon,-\varepsilon,\varepsilon,\varepsilon\right]$	$-(\alpha-\beta)$
$\Psi_7=\left[\frac{1}{\varepsilon},-\frac{1}{\varepsilon},\frac{1}{\varepsilon},-\frac{1}{\varepsilon},-\varepsilon,\varepsilon,-\varepsilon,\right]$	$-(\alpha-\beta)$
$\Psi_8=\left[\frac{1}{\varepsilon},-\frac{1}{\varepsilon},-\frac{1}{\varepsilon},\frac{1}{\varepsilon},-\varepsilon,\varepsilon,\varepsilon,-\varepsilon\right]$	$-(\alpha-\beta)$

$$\varepsilon^2=\frac{\beta}{J_{12}}+\left[\left(\frac{\beta}{J_{12}}\right)-1\right]^{1/2}, \tag{5.3}$$

thus

$$\frac{\beta}{J_{12}}=\frac{1}{2}\left[\varepsilon^2+\frac{1}{\varepsilon^2}\right]=\cosh(2\ln(\varepsilon)) . \tag{5.4}$$

The normalization factor for all eigenvectors is

$$\frac{1}{2}\left[\frac{J_{12}}{\beta}\right]^{1/2} . \tag{5.5}$$

Ψ_1 and Ψ_2 can be interpreted as ferromagnetic and ferrimagnetic modes of the system, respectively, where the intrasublattice alignment is ferromagnetic. Ψ_3, Ψ_4, and Ψ_5 correspond to degenerate modes where the A sublattice is aligned ferromagnetically with the B sublattice, with intrasublattice coupling being antiferromagnetic. Ψ_6, Ψ_7, and Ψ_8 have antiferromagnetic intersublattice and intrasublattice alignment.

The fourth-order term in the Landau free energy has the general form

$$\frac{u}{4}\frac{J_{12}^2}{\beta^2}\left[\tfrac{1}{2}(M_1^2+M_2^2)^2+(\delta_0+SM_1^2)^2+(\delta_0-SM_2^2)^2+\sum_{i=1}^{3}\left[(\delta_i+2Sa_i)^2+(\delta_i-2Sb_i)^2+2(a_i+b_i)^2\right]\right], \tag{5.6}$$

$$M_1^2=\Phi_1^2+\Phi_3^2+\Phi_4^2+\Phi_5^2=\Phi_1^2+m_1^2 , \tag{5.7a}$$

$$M_2^2=\Phi_2^2+\Phi_6^2+\Phi_7^2+\Phi_8^2=\Phi_2^2+m_2^2 , \tag{5.7b}$$

$$m_1^2=\Phi_3^2+\Phi_4^2+\Phi_5^2 , \tag{5.7c}$$

$$m_2^2=\Phi_6^2+\Phi_7^2+\Phi_8^2 , \tag{5.7d}$$

$$S=\frac{1}{2}\left[\varepsilon^2-\frac{1}{\varepsilon^2}\right]=\sinh[2\ln(\varepsilon)] , \tag{5.8}$$

$$\delta_0=\Phi_1\cdot\Phi_2+\Phi_3\cdot\Phi_6+\Phi_4\cdot\Phi_7+\Phi_5\cdot\Phi_8 , \tag{5.9a}$$

$$\delta_1=\Phi_1\cdot\Phi_6+\Phi_2\cdot\Phi_3+\Phi_4\cdot\Phi_8+\Phi_5\cdot\Phi_7 , \tag{5.9b}$$

$$\delta_2=\Phi_1\cdot\Phi_7+\Phi_2\cdot\Phi_4+\Phi_3\cdot\Phi_8+\Phi_5\cdot\Phi_6 , \tag{5.9c}$$

$$\delta_3=\Phi_1\cdot\Phi_8+\Phi_2\cdot\Phi_5+\Phi_3\cdot\Phi_7+\Phi_4\cdot\Phi_6 , \tag{5.9d}$$

$$a_1=\Phi_1\cdot\Phi_3+\Phi_4\cdot\Phi_5 , \tag{5.10a}$$

$$a_2=\Phi_1\cdot\Phi_4+\Phi_3\cdot\Phi_5 , \tag{5.10b}$$

$$a_3=\Phi_1\cdot\Phi_5+\Phi_3\cdot\Phi_4 , \tag{5.10c}$$

$$b_1=\Phi_2\cdot\Phi_6+\Phi_7\cdot\Phi_8 , \tag{5.11a}$$

$$b_2=\Phi_2\cdot\Phi_7+\Phi_6\cdot\Phi_8 , \tag{5.11b}$$

$$b_3=\Phi_2\cdot\Phi_8+\Phi_6\cdot\Phi_7 . \tag{5.11c}$$

We first minimize with respect to the δ's, a's, and b's obtaining a set of seven conditions on the relative angles of the normal modes and a greatly simplified form for the free energy

$$\delta_0=\frac{S}{2}(M_2^2-M_1^2) , \tag{5.12}$$

$$\delta_i=S(b_i-a_i),\quad i=1..3 \tag{5.13}$$

$$a_i+b_i=0,\quad i=1..3 \tag{5.14}$$

$$f(T,\mathbf{H})=\mu_0-2H\left[\left[\frac{\beta+J_{12}}{\beta}\right]^{1/2}\Phi_1+\left[\frac{\beta-J_{12}}{\beta}\right]^{1/2}\Phi_2\right]+\tfrac{1}{2}(r_1m_1^2+r_2m_2^2+r_1'\Phi_1^2+r_2'\Phi_2^2)+\frac{u}{4}(m_1^2+m_2^2+\Phi_1^2+\Phi_2^2)^2 , \tag{5.15}$$

where

$$r_1=n(T-T_c^1)=nT+\alpha+\beta , \tag{5.16a}$$

$$r_2=n(T-T_c^2)=nT+\alpha-\beta , \tag{5.16b}$$

$$r_1'=n(T-T_c^{1\prime})=nT-3(\alpha+\beta) , \tag{5.16c}$$

$$r_2'=n(T-T_c^{2\prime})=nT-3(\alpha-\beta) , \tag{5.16d}$$

$$T_c^{1\prime}=-3T_c^1 , \tag{5.17a}$$

$$T_c^{2\prime}=-3T_c^2 . \tag{5.17b}$$

As in the one-sublattice problem, there are no conditions determining the relative magnitudes of modes 3, 4, and 5, or modes 6, 7, and 8. Thus when either of m_1 or m_2 are magnetized, the internal two-dimensional degeneracy discussed in Sec. I will be present. Which r's are critical depends on the signs of α and β and also on whether or not $|\alpha| < |\beta|$. Figure 9 shows which regions of α,β space stabilize the $\mathbf{q}=\mathbf{0}$ modes. One can see that, for $\alpha < 0$ in a region where $|\alpha| > |\beta|$ the system is incommensurate or dispersionless. This leaves three essentially different cases to consider.

Case 1: $|\alpha| < |\beta|$, $\beta > 0$. Modes Φ_1 and m_2 order spontaneously. The order of the T_c's is determined by α,

$$0 < T_c^2 < T_c^{1\prime} \quad \text{for } \beta > \alpha > -\frac{\beta}{2} , \tag{5.18a}$$

$$0 < T_c^{1\prime} < T_c^2 \quad \text{for } -\frac{\beta}{2} > \alpha > -\beta . \tag{5.18b}$$

Case 2 : $|\alpha| < |\beta|$, $\beta < 0$. Modes Φ_2 and m_1 order spontaneously. The order of the T_c's is determined by α,

$$0 < T_c^1 < T_c^{2\prime} \quad \text{for } -\beta > \alpha > \frac{\beta}{2} , \tag{5.19a}$$

$$0 < T_c^{2\prime} < T_c^1 \quad \text{for } \frac{\beta}{2} < \alpha < \beta . \tag{5.19b}$$

Case 3: $|\alpha| > |\beta|$, $\alpha > 1$. Modes Φ_1 and Φ_2 order spontaneously. The order of the T_c's is determined by the sign of β,

$$0 < T_c^{1\prime} < T_c^{2\prime} \quad \text{for } \beta > 0 , \tag{5.20a}$$

$$0 < T_c^{2\prime} < T_c^{1\prime} \quad \text{for } \beta < 0 . \tag{5.20b}$$

In general, then, all these systems will have two transition temperatures, and thus rather complex behavior can be expected from magnetization and susceptibility measurements. As an example we have calculated the thermal evolution of the uniform magnetization at zero field by solving the mean-field equations (2.10) numerically. Figure 10 shows the results for $J_1 = -1$, $J_2 = \frac{1}{2}$, and $J_{12} = -1$, which corresponds to case 2 with $T_c^{2\prime} > T_c^1$. It is interesting to note that the numerical solutions of the mean-field equations (2.10) also show that the value of ε (which determines the relative magnetizations of the A and B sublattices) deviates very slightly from the value given in (5.3) and is temperature dependant.

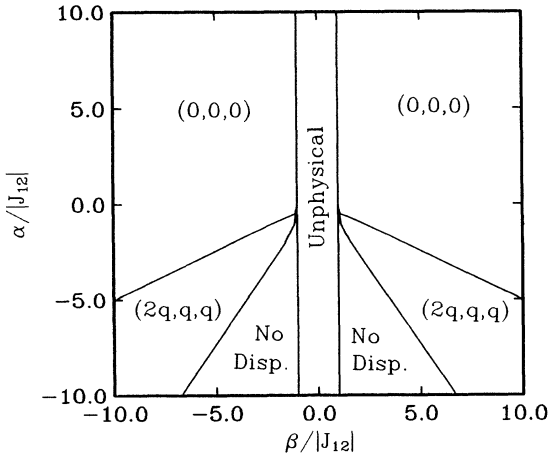

FIG. 9. Similar to Fig. 8 except parametrized in terms of α and β [defined in (5.1) and (5.2)] with $|J_{12}| = 1$.

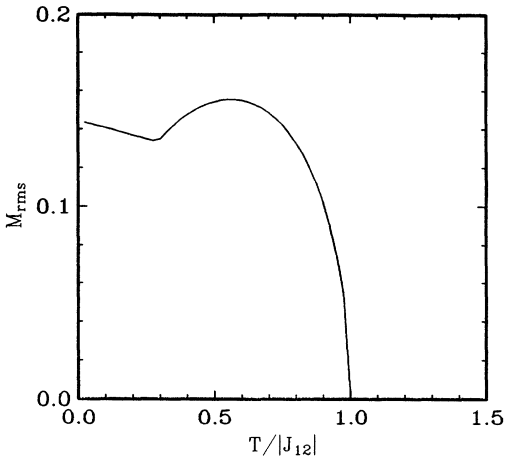

FIG. 10. Unusual temperature dependence of the uniform magnetization [calculated numerically from (2.10)] of a two-sublattice system with exchange parameters $J_1 = -1$, $J_2 = \frac{1}{2}$, and $J_{12} = -1$, corresponding to case 2 in Sec. V B.

CONCLUSIONS

The prevailing theme throughout this work has been the unusually high degree of degeneracy in the ordered phases of pyrochlores. These degeneracies are of two sorts, the first being the internal two-dimensional degeneracy with respect to the relative orientations of the sublattices for $\mathbf{q}=\mathbf{0}$ systems. In the Landau theory this degeneracy was revealed in the indeterminacy of the relative magnitudes of the three ordering modes Φ_1, Φ_2, and Φ_3. This sort of degeneracy is also present in type-I fcc antiferromagnets[15] but not in triangular systems at zero field. Mean-field analysis of the classical XY model on a triangular lattice[20] and classical dipoles on a honeycomb lattice[21] also show a one-dimensional internal degeneracy with respect to the relative orientations of the ordering sublattices.

The other type of degeneracy is the complete $\mathbf{q}$ independence of two of the eigenvalues of the coupling matrix for the NN one sublattice model. This means that for every possible $\mathbf{q}$ in the zone, there are two modes with the same free-energy independent of $\mathbf{q}$ (within the MF approximation). This degeneracy is macroscopic, and no long-range order is predicted within the MF approximation. For three-dimensional systems such dispersionless modes over the whole zone are so far unique to the corner-sharing tetrahedral lattice. No such degeneracy occurs for stacked triangular lattice systems. It is interesting to note that Rastelli and Tassi[22] have found that the so-called "rhombohedral antiferromagnet" is degenerate along certain lines in $\mathbf{q}$ space, which they call "degeneration lines." A similar sort of degeneracy occurs in

the fcc Ising antiferromagnet with NN interactions.[23] Further neighbor interactions in the pyrochlore system will in general select the $\mathbf{q}=\mathbf{0}$ or incommensurate phases. The same sort of degeneracies arise in the two-sublattice (both A and B are magnetic) pyrochlore systems. In particular, over a large region of coupling parameter space, the system is dispersionless along the $(0,q,q)$ direction.

The results for the Kagomé and square lattice with crossings are also of interest since a $\mathbf{q}$-independent mode is also present in these systems, and recent experimental work (neutron scattering,[24] magnetic susceptibility,[24,25] and heat capacity[25,26]) on the stacked kagomé lattice system $SrCr_8Ga_4O_{19}$ show spin-glass-like behavior. Another realization of the Kagomé lattice is ^{3}He adsorbed on graphite where the ^{3}He nuclear moments are coupled antiferromagnetic with isotropic symmetry. Heat-capacity measurements[27] show a cusplike peak; however, the entropy loss down to low temperatures is only half the expected value. Elser[28] has recently provided an explanation for this in which three-quarters of the spins form a singlet spin liquid and the other quarter are free.

One might expect that thermal fluctuations will reduce the degree of degeneracy in these systems. In fact through low-temperature expansions Larson and Henley[15] have shown that thermal fluctuations will select collinear ordered states in fcc antiferromagnets. Work is under way on the effects of thermal fluctuations in the pyrochlore system.

The mean-field calculations presented here are certainly consistent with (1) the observed long-range order in FeF_3, (2) the lack of long-range order in many other pyrochlores, and (3) some aspects of the unusual magnetization curves observed in $Nd_2Mo_2O_7$, $Sm_2Mo_2O_7$, and $Gd_2Mo_2O_7$.[7] The question remains as to whether the dispersionless modes are responsible for the spin-glass-like behavior observed in the chemically ordered compounds, $Y_2Mo_2O_7$ (Refs. 9 and 10) and $Tb_2Mo_2O_7$.[11] It is plausible that the liquidlike magnetic neutron scattering, observed in $Tb_2Mo_2O_7$, is a result of the presence of many degenerate modes with different $\mathbf{q}$'s along $(0,q,q)$. Other spin-glass-like properties, such as susceptibility cusps and sample history dependence cannot really be described within the mean-field approximation. They require a more sophisticated treatment. Low-temperature (≈ 1 K) neutron-diffraction experiments for many of the pyrochlore compounds would be interesting, particularly if some of the incommensurate phases predicted here could be observed. Many members of the $R_2Mn_2O_7$ and $R_2Mo_2O_7$ have not yet been investigated by neutron-diffraction or low-field susceptibility. Many of these compounds might be expected to show spin-glass-like properties or unusual magnetic structures. Heat-capacity data would also provide information on entropy loss due to short-range ordering and the nature of long-range order phase transitions when present.

From the evidence presented it is clear that the corner-sharing tetrahedral lattice is much more frustrated than the well-known stacked triangular lattice antiferromagnets. It is important to determine whether or not the spin-glass-like properties observed in these compounds are due to the frustration alone. It is generally believed that a spin glass must have some sort of chemical disorder; however, this does not seem to be the case in the pyrochlore compounds.[10] Answers to these questions may give some added insight into the role that frustration plays in the spin-glass problem.

ACKNOWLEDGMENTS

Personal communication with C. L. Henley concerning the fcc antiferromagnets is gratefully appreciated. We would also like to thank J. E. Greedan for a critical reading of the manuscript, providing computer facilities and many useful discussions. The Natural Sciences and Engineering Research Council of Canada is acknowledged for providing financial assistance for J. N. R. and operating funds for A. J. B. and A.-C. S.

APPENDIX A

Here we write out the matrix elements of the $J_{\mathbf{q}}^{ab}$ matrix, including the first four coordination shells of neighbors. Since the lattice is centro-symmetric $J_{\mathbf{q}}^{ab}$ is real and symmetric,

$$J_{\mathbf{q}}^{11}=J_{\mathbf{q}}^{22}=J_{\mathbf{q}}^{33}=J_{\mathbf{q}}^{44}=4J_3Q\ ,$$

where Q is defined in Eq. (4.2),

$$\begin{aligned}
J_{\mathbf{q}}^{12}=J_{\mathbf{q}}^{21}&=2J_1\cos(q_x)\\
&\quad+2J_2[\cos(2q_y-q_x)+\cos(2q_z-q_x)]\\
&\quad+4J_4\cos(2q_y-2q_z)\cos(q_x)\ ,\\
J_{\mathbf{q}}^{13}=J_{\mathbf{q}}^{31}&=2J_1\cos(q_y)\\
&\quad+2J_2[\cos(2q_z-q_y)+\cos(2q_x-q_y)]\\
&\quad+4J_4\cos(2q_z-2q_x)\cos(q_y)\ ,\\
J_{\mathbf{q}}^{14}=J_{\mathbf{q}}^{41}&=2J_1\cos(q_z)\\
&\quad+2J_2[\cos(2q_x-q_z)+\cos(2q_y-q_z)]\\
&\quad+4J_4\cos(2q_x-2q_y)\cos(q_z)\ ,\\
J_{\mathbf{q}}^{23}=J_{\mathbf{q}}^{32}&=2J_1\cos(q_x-q_y)\\
&\quad+2J_2[\cos(q_x+q_y)+\cos(2q_z-q_x-q_y)]\\
&\quad+4J_4\cos(q_x-q_y)\cos(2q_z)\ ,\\
J_{\mathbf{q}}^{24}=J_{\mathbf{q}}^{42}&=2J_1\cos(q_z-q_x)\\
&\quad+2J_2[\cos(q_z+q_x)\cos(2q_y-q_z-q_x)]\\
&\quad+4J_4\cos(q_z-q_x)\cos(2q_y)\ ,\\
J_{\mathbf{q}}^{34}=J_{\mathbf{q}}^{43}&=2J_1\cos(q_y-q_z)\\
&\quad+2J_2[\cos(q_y+q_z)+\cos(2q_x-q_y-q_z)]\\
&\quad+4J_4\cos(q_y-q_z)\cos(2q_x)\ .
\end{aligned}$$

APPENDIX B

In order to prove that (4.16) is exact to all orders in $(m^2+\Phi_4^2)$ note that at $\mathbf{q}=0$ we need only consider the

free energy in one unit cell. From the eigenvectors in Table V, (2.18), and conditions (4.11) one can show that

$$(B^a)^2=\tfrac{1}{4}\sum_i \Phi_i^2=\tfrac{1}{4}(m^2+\Phi_4^2), \quad a=1,2,3,4 \ . \tag{B1}$$

From (2.8) we can write down the free energy of one unit cell

$$f(T,\mathbf{H})=-\tfrac{1}{2}\sum_{a,b} J_0^{ab}\mathbf{B}^a\cdot\mathbf{B}^b+\mathbf{H}\cdot\sum_a \mathbf{B}^a-T\sum_a S(B^a) \ , \tag{B2}$$

$$=-2H\Phi_4-\frac{n}{2}T_c m^2+\tfrac{1}{2}(3nT_c-48j_3)\Phi_4^2 -4TS[\tfrac{1}{4}(m^2+\Phi_4^2)^{1/2}] \ , \tag{B3}$$

with equilibrium conditions

$$\left[-nT_c-\frac{T}{(m^2+\Phi_4^2)^{1/2}}S'\right]m=0 \ , \tag{B4}$$

$$\left[3nT_c-48j_3-\frac{T}{(m^2+\Phi_4^2)^{1/2}}S'\right]\Phi_4=2H \ , \tag{B5}$$

where

$$S'=\frac{\partial S}{\partial(m^2+\Phi_4^2)^{1/2}} \ . \tag{B6}$$

Finally when $m\neq 0$, conditions (B4) and (B5) give

$$\Phi_4=\frac{H}{(2nT_c-12j_3)} \ . \tag{B7}$$

[1]P. W. Anderson, Phys. Rev. **102**, 1008 (1956).

[2]J. Villain, Z. Phys. B **33**, 31 (1978).

[3]J. M. Hastings and L. M. Corliss, Phys. Rev. **102**, 1460 (1956); F. K. Lotgering, J. Phys. (Paris) Colloq. **32**, C1-34 (1971); R. Plumier, M. Leconte, A. Miedan-gros, and M. Sougi, Phys. Lett. **55A**, 239 (1975); J. Akimitzu, K. Siratori, G. Shirane, M. Iizumi, and T. Watanabe, J. Phys. Soc. Jpn. **44**, 172 (1977); C. Poole and H. A. Farach, Z. Phys. B **47**, 55 (1982); V. G. Vologin, Fiz. Tverd. Tela (Leningrad) **29**, 2323 (1987) [Sov. Phys—Solid State **29**, 1339 (1987)].

[4]R. Ballou, J. Deportes, R. Lemaire, Y. Nakamura, and B. Ouladdiaf, J. Magn. Magn. Mater. **70**, 129 (1987); R. Ballou, J. Deportes, R. Lemaire, and B. Ouladdiaf, J. Appl. Phys. **63**, 3487 (1988).

[5]G. Ferey, R. De Pape, M. Leblanc, and J. Pannetier, Rev. Chem. Minérale **23**, 474 (1986).

[6]H. W. J. Blote, R. F. Wielinga, and W. J. Huiskamp, Physica **43**, 549 (1968).

[7]M. Sato, X. Yan, and J. E. Greedan, Z. Anorg. Allg. Chem. **540/541**, 177 (1986).

[8]M. A. Subramanian, C. C. Torardi, D. C. Johnson, J. Pannetier, and A. W. Sleight, J. Solid State Chem. **72**, 24 (1988).

[9]J. E. Greedan, M. Sato, X. Yan, and F. S. Razavi, Solid State Commun. **59**, 895 (1986).

[10]J. N. Reimers and J. E. Greedan, J. Solid State Chem. **72**, 390 (1988).

[11]J. N. Reimers, J. E. Greedan, S. L. Penny and C. V. Stager, J. Appl. Phys. **67**, 5967 (1990).

[12]J. N. Reimers, J. E. Greedan, R. K. Kremer, E. Gmelin, and M. A. Subramanian (unpublished).

[13]J. E. Greedan, in *Magnetic Properties of Non-Metals,* Vol. III/27 of *Landolt-Börnstein New Series,* edited by H. P. J. Wijn (Springer, Berlin, in press).

[14]H. Kawamura, J. Phys. Soc. Jpn. **58**, 584 (1989).

[15]C. L. Henley, J. Appl. Phys. **61**, 3962 (1987); B. E. Larson and C. L. Henley (unpublished).

[16]P. Lacorre, J. Phys. C **20**, L775 (1987).

[17]A. B. Harris, O. G. Mouritson, and A. J. Berlinsky, Can. J. Phys. **62**, 915 (1984).

[18]E. F. Bertaut, J. Phys. Chem. Solids **21**, 256 (1961).

[19]For drawings of the Kagomé lattice and the square lattice with crossings, see R. Liebmann, *Statistical Mechanics of Periodic Frustrated Ising Systems* (Springer, Berlin, 1986), p. 27, Fig. (c) (Kagomé) and p. 28 Fig. (f) (square lattice with crossings). A discussion of antiferromagnetic ordering of Ising spins on these lattices can be found on p. 77 (Kagomé lattice), p. 106 (square lattice with crossings), and p. 117 (3D pyrochlore).

[20]D. H. Lee, R. G. Caflisch, J. D. Joannopoulos, and F. Y. Wu, Phys. Rev. B **29**, 2680 (1984).

[21]G. O. Zimmerman, A. K. Ibrahim, and F. Y. Wu, Phys. Rev. B **37**, 2059 (1988).

[22]E. Rastelli and A. Tassi, J. Phys. **C19**, L423 (1986); **21**, L35 (1988).

[23]A. Danielian, Phys. Rev. **133**, A1344 (1964).

[24]C. Broholm, G. Aeppli, G. P. Espinosa, and A. S. Cooper. J. Appl. Phys. **67**, 5799 (A) (1990).

[25]A. P. Ramirez, G. P. Espinosa, and A. S. Cooper, Phys. Rev. Lett. **64**, 2070 (1990).

[26]A. P. Ramirez, G. P. Espinosa, and A. S. Cooper (unpublished).

[27]D. S. Greywall and P. A. Busch, Phys. Rev. Lett. **62**, 1868 (1989).

[28]V. Elser, Phys. Rev. Lett. **62**, 2405 (1989).